

Effects of metal co-ordination geometry on self-assembly: a monomeric complex with trigonal prismatic metal co-ordination vs. tetrameric complexes with octahedral metal co-ordination

Rowena L. Paul, Angelo J. Amoroso, Peter L. Jones, Samantha M. Couchman, Zoe R. Reeves, Leigh H. Rees, John C. Jeffery, Jon A. McCleverty* and Michael D. Ward*

School of Chemistry, University of Bristol, Cantock's Close, Bristol, UK BS8 1TS.
 E-mail: mike.ward@bristol.ac.uk

Received 29th January 1999, Accepted 23rd March 1999

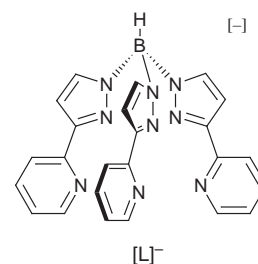
Complexes of Mn^{II} , Co^{II} and Zn^{II} with the hexadentate podand ligand tris[3-(2-pyridyl)pyrazol-1-yl]hydroborate $[L]^-$ have been prepared and structurally characterised. In mononuclear $[CoL][PF_6] \cdot CH_2Cl_2$ all three bidentate arms of the ligand are co-ordinated to the Co^{II} in a relatively strain-free manner to give a trigonal prismatic co-ordination geometry. In contrast in $[Mn_4L_4][PF_6]_4 \cdot 4MeCN \cdot Et_2O$ and $[Zn_4L_4][PF_6]_3[OH] \cdot 12EtOH$ the $[M_4L_4]^{4+}$ complex cations are tetrahedral clusters. Each ligand $[L]^-$ co-ordinates one bidentate arm to each of three metal ions in a $\kappa^2:\kappa^2:\kappa^2$ co-ordination mode, such that each ligand caps one triangular face of the metal tetrahedron. This trinucleating co-ordination mode, and the 1:1 correspondence of octahedral metal ions and hexadentate ligands, necessarily results in formation of the tetrahedral cluster in which all four metal tris(chelate) centres have the same chirality. Thus the mononucleating κ^6 co-ordination mode results when the metal ion can tolerate a trigonal prismatic geometry, whereas the trinucleating $\kappa^2:\kappa^2:\kappa^2$ mode occurs when the metal ions are octahedral. Spectroscopic evidence (1H NMR and UV/VIS spectroscopy and electrospray mass spectrometry, as appropriate) suggests that the monomeric and tetrameric forms are retained in solution and do not interconvert. Attempts to recrystallise $[Zn_4L_4][PF_6]_4$ from acetone–diethyl ether resulted in formation of a few crystals of the decomposition product $[Zn_4L_2(pypz)_2(\mu_4-PO_4)][PF_6]_3 \cdot 2Me_2CO \cdot 2Et_2O$ [pypz = 3-(2-pyridyl)pyrazole], in which $[L]^-$ adopts the hitherto unseen binucleating ($\kappa^4:\kappa^2$) co-ordination mode, the central bridging phosphate arising from hydrolysis of $[PF_6]^-$ under ambient conditions.

Introduction

It is now well established that architecturally complicated, high-nuclearity complexes can arise from self-assembly processes between relatively simple multidentate ligands and labile metal ions.¹ In a few cases careful control of the symmetry and flexibility of the ligands has led to the controlled assembly of complexes whose structures could be predicted in advance: these are exemplified by the molecular grids and cylinders of Lehn and co-workers,² and the molecular tetrahedra of Saalfrank *et al.*³ and Raymond and co-workers.^{4,5} More commonly the nature of the self-assembly process is not so predictable, because even when a ligand is designed with only one possible mode of co-ordination (*e.g.* bridging two metal centres by virtue of having two distinct binding sites) numerous different routes are possible for the assembly process, giving a range of products. This has been described as a ‘combinatorial library’, and is exemplified by recent reports from Constable⁶ and Lehn⁷ and their co-workers in which a single metal/ligand combination affords a variety of solid-state structures which interconvert in solution. An additional complicating factor in self-assembly processes may be that a ligand may adopt two or more different modes of co-ordination, as exemplified by (i) the linear oligopyridines, which can partition into bidentate or terdentate binding domains in several different ways according to the metal ion,⁸ and (ii) our recent report of a tetradentate ligand with two bidentate sites which can either span two metal ions or bind to a single metal ion to give completely different types of structure.⁹

We describe here the syntheses and crystal structures of complexes of the hexadentate podand ligand hydrotris[3-(2-pyridyl)pyrazol-1-yl]borate (KL), a derivative of the well

known tris(pyrazolyl)borate core¹⁰ in which each arm of the ligand is a bidentate chelate by virtue of the 2-pyridyl substituents attached to the C³ positions of the pyrazolyl rings. We have extensively developed the co-ordination chemistry of the ligand with lanthanide,^{11,12} transition-metal,^{13,14} and main-group metal ions.¹⁵ We demonstrate here how three different co-ordination modes (mononucleating, κ^6 ; bridging two metal ions, $\kappa^4:\kappa^2$; and bridging three metal ions, $\kappa^2:\kappa^2:\kappa^2$) are possible for this ligand with first-row transition-metal ions. We also demonstrate how the change from the mononucleating to the trinucleating mode results in different geometries at the metal centres and radically alters the assembly pathway to give tetrameric, rather than monomeric, complexes. A preliminary account of one of these structures has been published.¹³



Experimental

General details

The ligand KL was prepared as described earlier.¹¹ Electrospray (ES) mass spectra were recorded on a VG Quattro instrument,

fast atom bombardment (FAB) mass spectra on a VG Autospec instrument using 3-nitrobenzyl alcohol as matrix, ^1H NMR spectra at 400 MHz on a JEOL GX-400 spectrometer and electronic spectra on a Perkin-Elmer Lambda 19 instrument.

Preparations

All complexes were prepared by reaction of KL with the appropriate metal(II) acetate hydrate (1:1 ratio, on typically a 0.5 mmol scale) in MeOH to afford a clear solution, from which the complexes were precipitated on addition of aqueous KPF_6 . Yields were typically 50–60%. X-Ray quality crystals were grown from the following solvent mixtures: $[\text{CoL}][\text{PF}_6]\cdot\text{CH}_2\text{Cl}_2$ from CH_2Cl_2 –hexane; $[\text{Mn}_4\text{L}_4][\text{PF}_6]_4\cdot 4\text{MeCN}\cdot\text{Et}_2\text{O}$ from $\text{MeCN}\text{--}\text{Et}_2\text{O}$; $[\text{Zn}_4\text{L}_4][\text{PF}_6]_3[\text{OH}]\cdot 12\text{EtOH}$ from $\text{MeCN}\text{--}\text{EtOH}$. The complex $[\text{Zn}_4\text{L}_2(\text{pypz})_2(\mu_4\text{-PO}_4)][\text{PF}_6]_3\cdot 2\text{Me}_2\text{CO}\cdot 2\text{Et}_2\text{O}$ [pypz = 3-(2-pyridyl)pyrazole] was obtained as a trace decomposition product when $[\text{Zn}_4\text{L}_4][\text{PF}_6]_4$ was recrystallised from acetone– Et_2O . Analytical data for the complexes are given below; mass spectral data are discussed in the Results and discussion section. $[\text{CoL}][\text{PF}_6]$ (Found: C, 42.8; H, 3.3; N, 18.4. Required for $[\text{CoL}][\text{PF}_6]\cdot 0.5\text{CH}_2\text{Cl}_2$: C, 42.6; H, 2.9; N, 18.2%); electronic spectrum (in MeCN) λ_{max} 238 (ϵ 29 400), 282 (18 500), 491 (140) and 1136 nm ($10\text{ dm}^3\text{ mol}^{-1}\text{ cm}^{-1}$). $[\text{Mn}_4\text{L}_4][\text{PF}_6]_4$ (Found: C, 44.4; H, 3.0; N, 19.0. Required for $[\text{Mn}_4\text{L}_4][\text{PF}_6]_4$: C, 44.7; H, 3.0; N, 19.6%); electronic spectrum (in MeCN) λ_{max} 250 (ϵ 129 000) and 295 nm ($130\text{ 000 dm}^3\text{ mol}^{-1}\text{ cm}^{-1}$). $[\text{Zn}_4\text{L}_4][\text{PF}_6]_4$ (Found: C, 44.1; H, 3.4; N, 19.0. Required for $[\text{Zn}_4\text{L}_4][\text{PF}_6]_4$: C, 44.0; H, 2.9; N, 19.3%); electronic spectrum (in MeCN) λ_{max} 244 (ϵ 93 000) and 287 ($82\text{ 000 dm}^3\text{ mol}^{-1}\text{ cm}^{-1}$).

Crystallography

All of the crystals studied contained lattice solvent molecules. Consequently suitable crystals were mounted on the diffractometer either in a stream of cold N_2 (-100°C), or at room temperature in sealed glass capillary tubes containing some of the mother-liquor. A Siemens SMART three-circle diffractometer with a CCD area detector for $[\text{Mn}_4\text{L}_4][\text{PF}_6]_4\cdot 4\text{MeCN}\cdot\text{Et}_2\text{O}$, $[\text{CoL}][\text{PF}_6]\cdot\text{CH}_2\text{Cl}_2$ and $[\text{Zn}_4\text{L}_2(\text{pypz})_2(\text{PO}_4)][\text{PF}_6]_3\cdot 2\text{Me}_2\text{CO}\cdot 2\text{Et}_2\text{O}$, or a Siemens R3m/V four-circle diffractometer with a conventional point detector for $[\text{Zn}_4\text{L}_4][\text{PF}_6]_3[\text{OH}]\cdot 12\text{EtOH}$ was employed. A detailed experimental description of the methods used for data collection and integration using the SMART system has been published.¹¹ Graphite-monochromatised Mo-K α X-radiation ($\lambda = 0.71073\text{ \AA}$) was used in all cases. Details of the crystal parameters, data collection and refinement are summarised in Table 1. After integration of the data (for those data sets collected on the SMART system) and merging of equivalent reflections, empirical absorption corrections were applied. All structures were solved by conventional heavy-atom or direct methods, and refined by the full-matrix least-squares method using all F^2 data, with the SHELX suite of programs.¹⁶ Except where stated otherwise below, all non-hydrogen atoms were refined with anisotropic thermal parameters; hydrogen atoms were included in calculated positions and refined with isotropic thermal parameters riding on those of the parent atom.

The structural determination of $[\text{CoL}][\text{PF}_6]\cdot\text{CH}_2\text{Cl}_2$ presented no particular problems. In $[\text{Mn}_4\text{L}_4][\text{PF}_6]_4\cdot 4\text{MeCN}\cdot\text{Et}_2\text{O}$ the asymmetric unit contains one entire complex unit, which therefore has no imposed symmetry, as well as four molecules of MeCN and one of diethyl ether to which geometric restraints were applied.

Crystals of $[\text{Zn}_4\text{L}_4][\text{PF}_6]_3[\text{OH}]\cdot 12\text{EtOH}$ diffracted very weakly. In contrast to the manganese(II) analogue, the tetranuclear complex cation $[\text{Zn}_4\text{L}_4]^{4+}$ lies on a threefold axis, such that the asymmetric unit contains one unique metal ion $[\text{Zn}(1)]$ and one on a threefold axis $[\text{Zn}(2)]$. There are therefore six complete molecules in the unit cell which has 18 asymmetric

units. Given the 4+ charge of the complex cation, we would expect to find one and a third anions in the asymmetric unit. In fact we found only one complete hexafluorophosphate anion, as well as collections of electron-density peaks which approximate to four molecules of EtOH. It was not possible to distinguish between the terminal C and O atoms, and all of the solvent atoms were refined as carbon atoms with isotropic thermal parameters. Hydrogen atoms for these solvent molecules were not included in the refinement. There was no trace of an additional $[\text{PF}_6]^-$ ion on a threefold axis, and we therefore assume that the missing anion is a low molecular weight anion which cannot be located because it is mixed up with the disordered solvent molecules. Obvious candidates are hydroxide or fluoride (the latter from decomposition of hexafluorophosphate); since these have the same molecular weight and scattering power we arbitrarily chose hydroxide to include in the calculations for density, absorption correction and so on. The problems with locating this fourth anion, and the large number of solvent molecules, are reflected in the modest quality of the refinement ($R1 = 0.0828$), but the structure of the tetranuclear complex cation is clearly defined with reasonable estimated standard deviation (e.s.d.) values for the metric parameters.

The tetranuclear complex cation in $[\text{Zn}_4\text{L}_2(\text{pypz})_2(\mu_4\text{-PO}_4)][\text{PF}_6]_3\cdot 2\text{Me}_2\text{CO}\cdot 2\text{Et}_2\text{O}$ lies on a C_2 axis passing through the phosphate P atom such that half of it is unique. The asymmetric units also contain 1.5 hexafluorophosphate ions (one complete, and one on a C_2 axis) as well as one molecule of acetone and one of ether. The atoms of these solvent molecules exhibit large thermal parameters, but it was not possible to resolve any disorder. Restraints were applied both to the geometries of the solvent molecules and to their thermal parameters to keep the refinement stable.

CCDC reference number 186/1404.

See <http://www.rsc.org/suppdata/dt/1999/1563/> for crystallographic files in .cif format.

Results and discussion

The monomeric complex $[\text{CoL}][\text{PF}_6]$

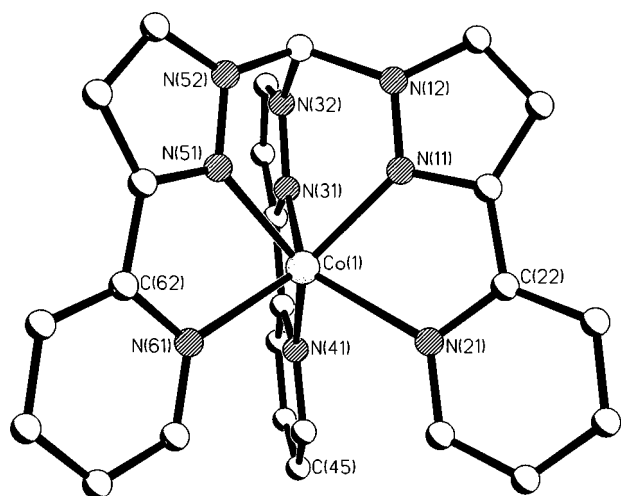
Reaction of KL with cobalt(II) acetate in MeOH afforded a clear pink solution, from which a pink solid precipitated on addition of aqueous KPF_6 . Elemental analysis and both FAB and electrospray mass spectrometry suggested a 1:1 metal to ligand ratio, giving the empirical formulation $[\text{CoL}][\text{PF}_6]$, which would be expected for a complex of a hexadentate ligand with a metal ion that is commonly pseudo-octahedral. However simple molecular modelling studies showed that adoption of an octahedral geometry about the metal centre in a 1:1 complex would involve considerable ligand strain. The ligand naturally tends to adopt a conformation in which the six donor atoms are in a trigonal prismatic array, and rearrangement of this to present an octahedral donor set to a metal would require a substantial degree of twisting of the ligand to make the plane of the three pyrazolyl donors and the plane of the three pyridyl donors mutually staggered.

The crystal structure of the complex (Fig. 1, Table 2) shows that this problem is not an issue because the complex has trigonal prismatic geometry about the cobalt(II) centre with the ligand co-ordinating in a relatively undistorted manner. The three Co–N(pyrazolyl) bonds (average 2.06 Å) are significantly shorter than the three Co–N(pyridyl) bonds (average 2.27 Å) because of the divergent geometry of the three arms. In order to allow the pyridyl donors to approach the small metal ion within reasonable bonding distance, this divergence is minimised by a compression of the apical N–B–N angles (average 106.6°) compared to an ideal tetrahedral geometry. In contrast, in complexes of $[\text{L}]^-$ with lanthanide ions the apical N–B–N angles are more opened out ($\approx 109\text{--}110^\circ$), which permits the

Table 1 Crystallographic data for the four crystal structures

	[Mn ₄ L ₄][PF ₆] ₄ ·4MeCN·Et ₂ O	[Zn ₄ L ₄][PF ₆] ₃ [OH]·12EtOH	[CoL][PF ₆] ₃ ·CH ₂ Cl ₂	[Zn ₄ L ₂ (pypz) ₂ (PO ₄)][PF ₆] ₃ ·2Me ₂ CO·2Et ₂ O
Formula	C ₁₀₈ H ₉₈ B ₄ F ₂₄ Mn ₄ N ₄₀ OP ₄	C ₁₂₀ H ₁₄₉ B ₄ F ₁₈ N ₃₆ O ₁₃ P ₃ Zn ₄	C ₂₅ H ₂₁ BCl ₂ CoF ₆ N ₉ P	C ₇₈ H ₈₄ B ₂ F ₁₈ N ₂₄ O ₈ P ₄ Zn ₄
<i>M</i>	2815.14	3043.38	733.12	2234.67
System, space group	Monoclinic, <i>P</i> 2 ₁ / <i>n</i>	Trigonal, <i>R</i> 3̄	Triclinic, <i>P</i> 1̄	Monoclinic, <i>C</i> 2/ <i>c</i>
<i>T</i> /K	293	293	173	173
<i>a</i> /Å	21.778(8)	26.528(6)	11.240(2)	18.291(2)
<i>b</i> /Å	20.352(6)	26.528(6)	12.224(3)	22.321(3)
<i>c</i> /Å	28.898(9)	36.863(13)	12.359(3)	24.103(3)
<i>α</i> /°			62.36(2)	
<i>β</i> /°	103.83(3)		77.69(2)	104.946(13)
<i>γ</i> /°			85.73(2)	
<i>U</i> /Å ³	12437(7)	22466(11)	1469.2(6)	9508(2)
<i>Z</i>	4	6	2	4
<i>D</i> _c /g cm ⁻³	1.503	1.350	1.657	1.561
<i>μ</i> /mm ⁻¹	0.55	0.754	0.894	1.165
Crystal size/mm	0.75 × 0.75 × 0.60	0.25 × 0.25 × 0.30	0.16 × 0.16 × 0.04	0.4 × 0.4 × 0.4
2θ limit for data collection/°	46.5	45	50	50
Reflections collected: total, independent, <i>R</i> _{int}	42954, 17194, 0.0565	7038, 6532, 0.0375	12659, 5160, 0.0833	24571, 8328, 0.0610
Data, restraints, parameters	17194, 46, 1673	6469, 0, 534	5128, 0, 406	8301, 102, 623
Final <i>R</i> 1, <i>wR</i> 2 ^{<i>a</i>,<i>b</i>}	0.0643, 0.1690	0.0828, 0.2662	0.0737, 0.2078	0.0592, 0.1643
Weighting factors ^{<i>b</i>}	0.0650, 22.48	0.1480, 70.70	0.1066, 0	0.0767, 20.1303
Largest residuals/e Å ⁻³	+0.652, -0.522	+0.659, -0.410	+0.765, -1.046	+0.787, -0.670

^{*a*} Structure was refined on *F*_o² using all data; the value of *R*1 is given for comparison with older refinements based on *F*_o with a typical threshold of *F* ≥ 4σ(*F*). ^{*b*} *wR*2 = [Σ*w*(*F*_o² - *F*_c²)/Σ*w*(*F*_o²)^{1/2}]² where *w*⁻¹ = σ²(*F*_o²) + (*aP*)² + *bP* and *P* = [max(*F*_o², 0) + 2*F*_c²]/3.

**Fig. 1** Crystal structure of the complex cation of [CoL][PF₆]₃·CH₂Cl₂.

greater metal-to-ligand distances that are required.¹¹ Trigonal prismatic co-ordination geometry is less favoured than octahedral on steric grounds, and in addition LFSE effects favour octahedral geometries for most d-electron configurations (obvious exceptions being d⁰, high-spin d⁵ and d¹⁰, where LFSE is zero in all geometries).¹⁷ It is accordingly relatively rare, and tends to occur only when there is an element of rigidity in the ligand donor set which imposes trigonal pyramidal geometry,¹⁸ as is clearly the case for [CoL][PF₆].

Complexes of Co^{II} are almost always high spin; this was confirmed for [CoL][PF₆] by a room-temperature magnetic susceptibility measurement of 3.7 μ_B. We note that the low energy of the first d-d transition (1136 nm) is consistent with the trigonal prismatic geometry being retained in solution, because trigonal prismatic cobalt(II) complexes have lower-energy d-d transitions than octahedral complexes with the same donor sets.¹⁹ Given that the bidentate pyrazolopyridine 'arm' of [L]⁻ has a very similar ligand-field strength to that of 2,2'-bipyridine,²⁰ a complex between Co^{II} and [L]⁻ in which the metal ion was octahedral would be expected to have its lowest-energy d-d transition at about the same position as that of [Co(bipy)₃]²⁺ (885 nm).

Table 2 Selected bond lengths [Å] and angles [°] for [CoL][PF₆]₃·CH₂Cl₂

Co(1)–N(31)	2.060(5)	Co(1)–N(61)	2.259(5)
Co(1)–N(11)	2.061(5)	Co(1)–N(21)	2.281(5)
Co(1)–N(51)	2.066(6)	Co(1)–N(41)	2.284(5)
N(31)–Co(1)–N(11)	80.7(2)	N(51)–Co(1)–N(21)	128.1(2)
N(31)–Co(1)–N(51)	80.6(2)	N(61)–Co(1)–N(21)	97.5(2)
N(11)–Co(1)–N(51)	80.3(2)	N(31)–Co(1)–N(41)	72.4(2)
N(31)–Co(1)–N(61)	127.6(2)	N(11)–Co(1)–N(41)	127.7(2)
N(11)–Co(1)–N(61)	134.5(2)	N(51)–Co(1)–N(41)	135.2(2)
N(51)–Co(1)–N(61)	72.2(2)	N(61)–Co(1)–N(41)	96.9(2)
N(31)–Co(1)–N(21)	133.9(2)	N(21)–Co(1)–N(41)	95.8(2)
N(11)–Co(1)–N(21)	72.0(2)		

Tetrameric complexes [M₄L₄][PF₆]₄ (M = Mn or Zn)

Reaction of KL with manganese(II) or zinc(II) acetate in MeOH in a 1 : 1 ratio afforded clear solutions from which off-white solids precipitated on addition of aqueous KPF₆. Elemental analyses again suggested a 1 : 1 metal to ligand ratio, giving the empirical formulations [ML][PF₆]. Although the FAB mass spectra in each case showed peaks corresponding to mononuclear [ML]⁺ fragments, the electrospray mass spectra each showed a weak peak corresponding to tetranuclear species [M₄L₄(PF₆)₃]³⁺ (for M = Mn, *m/z* = 714; for M = Zn, *m/z* = 727). Thus the electrospray spectra of the complexes of Mn^{II} and Zn^{II} both showed evidence for formation of tetramers, which the electrospray mass spectrum of [CoL][PF₆] did not.

The crystal structures of the two complexes confirm the formation of the unusual tetranuclear complex cations [M₄L₄]⁴⁺ (M = Mn or Zn; Figs. 2–4). The two complex cations have very similar structures, the principal difference being that in the [Mn₄L₄]⁴⁺ cation all four metal ions are crystallographically independent, whereas the [Zn₄L₄]⁴⁺ cation lies on a threefold axis which passes through Zn(2) and the centre of the face described by Zn(1), Zn(1A) and Zn(1B). Selected metric parameters for the two structures are in Tables 3 and 4. Each ligand is spread out such that it co-ordinates each of its three bidentate arms to a different metal ion, *i.e.* it caps one triangular face of the metal tetrahedron. In order to do this, the tris(pyrazolyl)borate fragment adopts an unusual 'inverted' geometry such that the apical hydride is directed inwards,

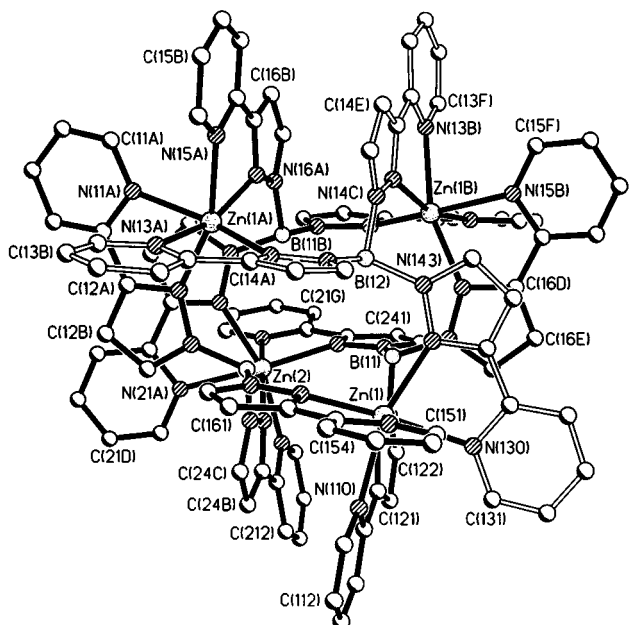


Fig. 2 Crystal structure of the complex cation of $[Zn_4L_4][PF_6]_3[OH] \cdot 12EtOH$; one ligand is drawn with clear bonds.

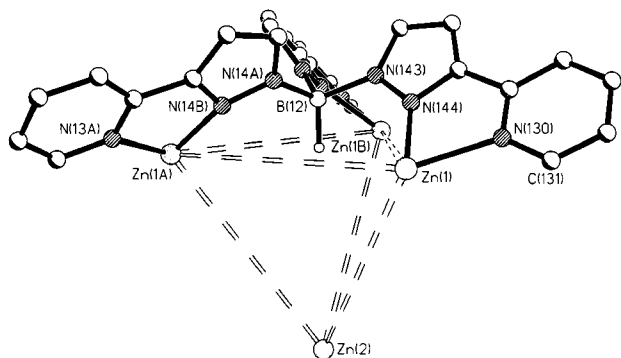


Fig. 3 View of part of the complex cation of $[Zn_4L_4][PF_6]_3[OH] \cdot 12EtOH$, emphasising the co-ordination mode of each ligand.

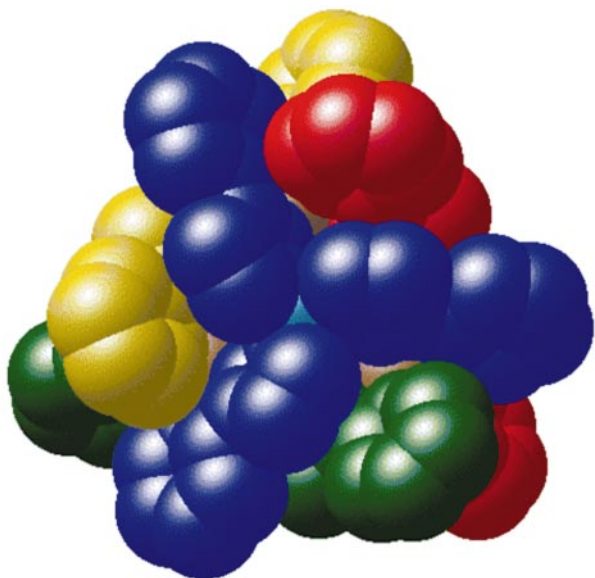


Fig. 4 Space-filling view of the complex cation of $[Mn_4L_4][PF_6]_4 \cdot 4MeCN \cdot Et_2O$ with each ligand coloured differently.

towards the centre of the triangular face (Fig. 3). This conformation appears to be necessary for all three pyrazolyl donors to co-ordinate to different atoms, rather than converging on one atom.²¹ Each metal ion is therefore in a pseudo-octahedral

co-ordination geometry, arising from three bidentate pyrazolylpyridine groups provided by three different ligands, in contrast to the trigonal prismatic co-ordination geometry seen for $[CoL][PF_6]$. A space-filling picture (Fig. 4) shows how the intermeshing of the four ligands leads to numerous aromatic π -stacking interactions between overlapping sections of different ligands. All four metal ions have the same chirality, which is essential for steric reasons; the four ligands could not interlock without interference between them if any one of the metals had a different configuration from the others.

It is apparent that formation of this tetrameric structure is the only way in which an octahedral geometry can be attained with this ligand: since it is not possible for the three arms of one ligand to provide an octahedral donor set to one encapsulated metal ion, it is necessary to use three independent bidentate fragments, one from each of three different ligands. With the benefit of hindsight we can see how this necessarily leads to formation of a tetrahedron. Each ligand, because it binds to three different metals, can be considered to cap a triangular face of a polyhedron which has metal ions at its vertices. Each vertex is likewise connected to three faces (*i.e.* each metal interacts with three bidentate ligand arms to give the required octahedral geometry). Given a 1:1 metal:ligand stoichiometry, because each ligand has six donor atoms and each metal requires six donors, we require a polyhedron having the same number of (three-connected) vertices as (triangular) faces, *i.e.* a tetrahedron having 4 vertices and 4 faces. This symmetry-based argument has recently been exploited by Raymond for the planned synthesis of topologically similar tetrahedral complexes with a 4:4 metal:ligand ratio;⁵ as far as we know, these are the only other examples of complexes with this topology.

Possible monomer/tetramer equilibrium

The contrast between the structures of $[CoL]^+$ and $[M_4L_4]^{4+}$ ($M = Mn$ or Zn) is surprising. Since both Mn^{II} and Zn^{II} have no stereoelectronic preferences arising from partially filled d shells, whereas high-spin Co^{II} has a definite preference for octahedral geometry over trigonal prismatic, we might expect to see the alternate forms of the structures: *i.e.* trigonal prismatic monomers for Mn^{II} and Zn^{II} , but octahedral tetramers for Co^{II} . The fact that this is not the case suggests that the balance between the two forms is very fine, such that there might be an equilibrium mixture of the two in solution which, on crystallisation, all converts into whichever form crystallises preferentially.

To investigate this possibility further we looked at the solution NMR spectrum of the diamagnetic zinc(II) complex. The 1H NMR spectrum of $[Zn_4L_4][PF_6]_4$ in d^6 -acetone at room temperature showed only six aromatic resonances, all of the same intensity and clearly ascribable to the four pyridyl and two pyrazolyl protons of each bidentate arms. Whilst this is exactly consistent with the crystal structure, in which all bidentate arms of all ligands are equivalent, it could also be consistent with a trigonal prismatic monomeric structure having threefold symmetry. However any exchange in solution between the two forms, if occurring, would almost certainly be slow on the NMR timescale because of the large amount of rearrangement involved; the presence of an equilibrium between two forms in solution would therefore show two sets of signals, which is not the case. In addition the electrospray mass spectrum of a solution of $[CoL][PF_6]$ showed no evidence for tetramer formation, in contrast to the mass spectra of the complexes of Mn^{II} and Zn^{II} . Finally, as mentioned above the unusually low energy for the first d-d transition of $[CoL]^+$ is suggestive of trigonal prismatic co-ordination in solution. All of the evidence suggests therefore that the solution structures are essentially the same as the crystal structures in each case.

Crystal structure of the by-product $[Zn_4L_2(pyppz)_2(\mu_4-PO_4)][PF_6]_3$

Although we could successfully grow crystals of $[Zn_4L_4][PF_6]_3$ -

Table 3 Selected bond lengths [Å] and angles [°] for [Mn₄L₄][PF₆]₄·4MeCN·Et₂O

Mn(1)–N(111)	2.222(4)	Mn(2)–N(131)	2.224(4)	Mn(3)–N(231)	2.233(4)	Mn(4)–N(411)	2.256(4)
Mn(1)–N(121)	2.338(4)	Mn(2)–N(461)	2.336(4)	Mn(3)–N(321)	2.339(5)	Mn(4)–N(421)	2.350(4)
Mn(1)–N(351)	2.251(4)	Mn(2)–N(451)	2.257(4)	Mn(3)–N(311)	2.251(4)	Mn(4)–N(251)	2.216(4)
Mn(1)–N(361)	2.347(4)	Mn(2)–N(141)	2.378(4)	Mn(3)–N(241)	2.354(4)	Mn(4)–N(261)	2.333(4)
Mn(1)–N(431)	2.256(4)	Mn(2)–N(211)	2.257(4)	Mn(3)–N(151)	2.254(4)	Mn(4)–N(341)	2.319(4)
Mn(1)–N(441)	2.304(4)	Mn(2)–N(221)	2.324(4)	Mn(3)–N(161)	2.329(5)	Mn(4)–N(331)	2.271(4)
N(111)–Mn(1)–N(351)	106.74(14)	N(131)–Mn(2)–N(451)	109.95(14)	N(231)–Mn(3)–N(311)	109.36(14)	N(251)–Mn(4)–N(411)	108.74(14)
N(111)–Mn(1)–N(441)	159.9(2)	N(131)–Mn(2)–N(221)	157.10(14)	N(231)–Mn(3)–N(161)	157.5(2)	N(251)–Mn(4)–N(341)	158.5(2)
N(111)–Mn(1)–N(121)	73.22(14)	N(131)–Mn(2)–N(461)	89.88(14)	N(231)–Mn(3)–N(321)	90.4(2)	N(251)–Mn(4)–N(261)	73.8(2)
N(441)–Mn(1)–N(121)	86.7(2)	N(221)–Mn(2)–N(461)	86.7(2)	N(161)–Mn(3)–N(321)	87.3(2)	N(341)–Mn(4)–N(261)	84.7(2)
N(431)–Mn(1)–N(361)	162.59(14)	N(211)–Mn(2)–N(141)	91.98(14)	N(151)–Mn(3)–N(241)	90.6(2)	N(331)–Mn(4)–N(421)	160.7(2)
N(111)–Mn(1)–N(431)	106.75(14)	N(131)–Mn(2)–N(211)	108.79(14)	N(231)–Mn(3)–N(151)	107.79(14)	N(251)–Mn(4)–N(331)	106.2(2)
N(351)–Mn(1)–N(441)	91.7(2)	N(451)–Mn(2)–N(221)	90.61(14)	N(311)–Mn(3)–N(161)	91.3(2)	N(411)–Mn(4)–N(341)	91.2(2)
N(351)–Mn(1)–N(121)	159.9(2)	N(451)–Mn(2)–N(461)	72.70(14)	N(311)–Mn(3)–N(321)	72.4(2)	N(411)–Mn(4)–N(261)	158.6(2)
N(111)–Mn(1)–N(361)	88.1(2)	N(131)–Mn(2)–N(141)	72.62(14)	N(231)–Mn(3)–N(241)	72.9(2)	N(251)–Mn(4)–N(421)	90.6(2)
N(441)–Mn(1)–N(361)	90.1(2)	N(221)–Mn(2)–N(141)	84.6(2)	N(161)–Mn(3)–N(241)	84.6(2)	N(341)–Mn(4)–N(421)	87.9(2)
N(351)–Mn(1)–N(431)	110.45(14)	N(451)–Mn(2)–N(211)	106.41(14)	N(311)–Mn(3)–N(151)	107.49(14)	N(411)–Mn(4)–N(331)	110.10(14)
N(431)–Mn(1)–N(441)	72.81(14)	N(211)–Mn(2)–N(221)	73.18(14)	N(151)–Mn(3)–N(161)	72.9(2)	N(331)–Mn(4)–N(341)	73.0(2)
N(431)–Mn(1)–N(121)	88.3(2)	N(211)–Mn(2)–N(461)	159.87(14)	N(151)–Mn(3)–N(321)	160.1(2)	N(331)–Mn(4)–N(261)	88.8(2)
N(351)–Mn(1)–N(361)	72.6(2)	N(451)–Mn(2)–N(141)	158.77(14)	N(311)–Mn(3)–N(241)	159.4(2)	N(411)–Mn(4)–N(421)	71.9(2)
N(121)–Mn(1)–N(361)	87.3(2)	N(461)–Mn(2)–N(141)	86.4(2)	N(321)–Mn(3)–N(241)	87.2(2)	N(261)–Mn(4)–N(421)	87.0(2)

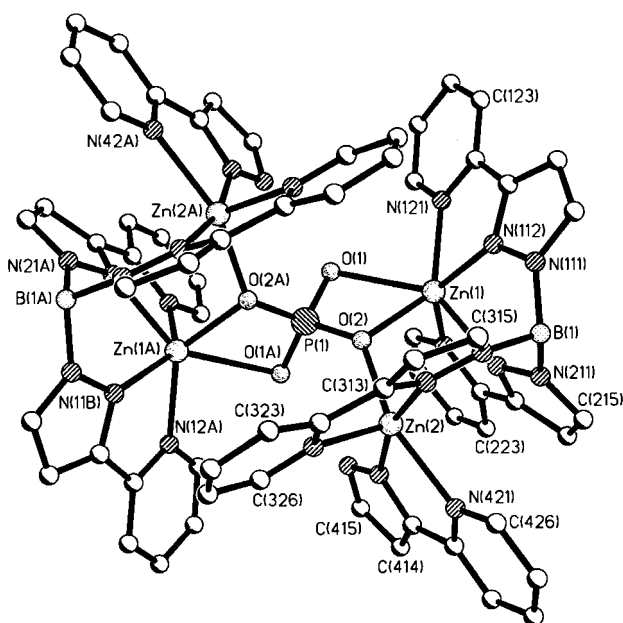
Table 4 Selected bond lengths [Å] and angles [°] for [Zn₄L₄][PF₆]₃·[OH]·12EtOH

Zn(1)–N(164)	2.126(6)	Zn(1)–N(110)	2.269(7)
Zn(1)–N(144)	2.146(7)	Zn(1)–N(150)	2.272(7)
Zn(1)–N(124)	2.149(6)	Zn(2)–N(244)	2.134(6) ^a
Zn(1)–N(130)	2.246(7)	Zn(2)–N(210)	2.270(6) ^b
N(164)–Zn(1)–N(144)	106.7(2)	N(164)–Zn(1)–N(150)	75.5(2)
N(164)–Zn(1)–N(124)	107.9(2)	N(144)–Zn(1)–N(150)	90.4(3)
N(144)–Zn(1)–N(124)	106.5(2)	N(124)–Zn(1)–N(150)	160.4(3)
N(164)–Zn(1)–N(130)	160.4(2)	N(130)–Zn(1)–N(150)	85.0(3)
N(144)–Zn(1)–N(130)	75.6(3)	N(110)–Zn(1)–N(150)	85.9(3)
N(124)–Zn(1)–N(130)	89.6(2)	N(244A)–Zn(2)–N(244)	106.7(2) ^a
N(164)–Zn(1)–N(110)	89.5(3)	N(244A)–Zn(2)–N(210)	162.0(2) ^{a,b}
N(144)–Zn(1)–N(110)	161.9(2)	N(244B)–Zn(2)–N(210)	75.4(2) ^{a,b}
N(124)–Zn(1)–N(110)	74.9(3)	N(244)–Zn(2)–N(210)	89.2(2) ^{a,b}
N(130)–Zn(1)–N(110)	86.4(3)	N(210)–Zn(2)–N(210A)	86.9(2) ^b

^a N(244) has symmetry equivalents N(244A) and N(244B). ^b N(210) has symmetry equivalents N(210A) and N(210B).

[OH]·12EtOH from a mixture of ethanol and acetonitrile, attempts to get better quality crystals from other solvent combinations (usually acetone–ether) occasionally afforded a few crystals of a different habit. Structural characterisation of these showed them to be an unusual decomposition product [Zn₄L₂(pypz)₂(μ₄-PO₄)] [PF₆]₃·2Me₂CO·2Et₂O (Fig. 5, Table 5). The structure consists of two {Zn₂L(pypz)}³⁺ units, in which the ligand [L][−] bridges two zinc(II) centres by co-ordinating two of its bidentate arms to one metal [Zn(1)] and one to the other [Zn(2)]. Also attached to Zn(2) is a bidentate ligand 3-(2-pyridyl)pyrazole (pypz), which must have been generated from [L][−] by B–N bond cleavage. Such decomposition of tris-(pyrazolyl)borates to liberate pyrazoles is common. The two {Zn₂L(pypz)}³⁺ units are linked by a bridging phosphate group, which is co-ordinated in such a way that two of its oxygen atoms, O(1) and its symmetry equivalent O(1A), co-ordinate to one metal [Zn(1) and Zn(1A) respectively], whereas the other two [O(2) and O(2A)] each bridge the pair of metal atoms Zn(1) and Zn(2) within each dinuclear {Zn₂L(pypz)}³⁺ unit. Atom Zn(1) is consequently five-co-ordinate, with an approximately square-based pyramidal geometry, whereas Zn(2) is six-co-ordinate. Aromatic stacking interactions are again evident, between the bidentate arm containing N(211) and N(221) attached to Zn(1), and the bidentate arm containing N(411) and N(421) attached to Zn(2).

Two features of this structure are of interest. First, this is the first time that we have observed [L][−] bridging two metal centres,

**Fig. 5** Crystal structure of the complex cation of [Zn₄L₂(pypz)₂(μ₄-PO₄)] [PF₆]₃·2Me₂CO·2Et₂O.**Table 5** Selected bond lengths [Å] and angles [°] for [Zn₄L₂(pypz)₂(PO₄)] [PF₆]₃·2Me₂CO·2Et₂O

Zn(1)–O(2)	2.067(4)	Zn(2)–O(2)	2.037(4)
Zn(1)–N(112)	2.124(4)	Zn(2)–N(412)	2.069(4)
Zn(1)–N(221)	2.151(4)	Zn(2)–N(312)	2.076(4)
Zn(1)–N(121)	2.190(4)	Zn(2)–N(321)	2.091(5)
Zn(1)–N(212)	2.198(4)	Zn(2)–N(421)	2.225(5)
Zn(1)–O(1)	2.462(4)		
O(2)–Zn(1)–N(112)	113.4(2)	O(2)–Zn(2)–N(412)	98.7(2)
O(2)–Zn(1)–N(221)	98.5(2)	O(2)–Zn(2)–N(312)	91.6(2)
N(112)–Zn(1)–N(221)	137.3(2)	N(412)–Zn(2)–N(312)	165.6(2)
O(2)–Zn(1)–N(121)	133.6(2)	O(2)–Zn(2)–N(321)	100.9(2)
N(112)–Zn(1)–N(121)	75.1(2)	N(412)–Zn(2)–N(321)	108.2(2)
N(221)–Zn(1)–N(121)	103.2(2)	N(312)–Zn(2)–N(321)	79.5(2)
O(2)–Zn(1)–N(212)	87.9(2)	O(2)–Zn(2)–N(421)	157.7(2)
N(112)–Zn(1)–N(212)	78.6(2)	N(412)–Zn(2)–N(421)	75.8(2)
N(221)–Zn(1)–N(212)	74.9(2)	N(312)–Zn(2)–N(421)	90.9(2)
N(121)–Zn(1)–N(212)	137.2(2)	N(321)–Zn(2)–N(421)	101.4(2)
O(2)–Zn(1)–O(1)	63.38(13)	N(121)–Zn(1)–O(1)	77.70(14)
N(112)–Zn(1)–O(1)	132.9(2)	N(212)–Zn(1)–O(1)	142.89(14)
N(221)–Zn(1)–O(1)	86.0(2)		

as opposed to bridging three metals (*cf.* $[M_4L_4][PF_6]_4$ above) or encapsulating a single metal (*cf.* $[CoL][PF_6]$ above and several lanthanide complexes). Secondly, the bridging phosphate anion must have arisen from hydrolysis of a hexafluorophosphate anion. Partial hydrolysis of hexafluorophosphate is known to give the difluorophosphate anion $[PO_2F_2]^-$, and there are several examples of crystal structures in which this anion occurs unexpectedly.²² Complete hydrolysis of hexafluorophosphate to phosphate usually requires vigorous conditions and is slow: catalysis by highly charged cations such as Th^{IV} , Zr^{IV} and Al^{III} has been observed.²³ There is however one recent example of the complete hydrolysis of hexafluorophosphate to phosphate which, like this new example, occurred under ambient conditions and was presumably assisted by transient co-ordination to a Lewis-acidic metal centre.²⁴ We note also that whilst examples of the phosphate ion bridging four metals are common in polyoxometalates and layered infinite sheets,²⁵ there is only one other example of this co-ordination mode in a molecular species.²⁴

Conclusion

Whereas the hexadentate ligand $[L]^-$ forms a mononuclear trigonal-prismatic complex $[CoL]^+$ with Co^{II} , the adoption of octahedral co-ordination geometries about Mn^{II} and Zn^{II} necessarily results in the formation of tetrameric complexes $[M_4L_4]^{4+}$ in which each ligand co-ordinates one bidentate arm to each of three metal ions, thereby forming a tetrahedral cluster with each ligand face-capping. The switch from the mononucleating (κ^6) to the trinucleating ($\kappa^2:\kappa^2:\kappa^2$) co-ordination modes, and the concomitant change from monomeric to tetrameric complex structures, therefore appears to be driven by the requirement of the metal ion for trigonal prismatic or octahedral co-ordination, respectively. Various pieces of spectroscopic evidence suggest that the monomeric cobalt(II) and tetrameric manganese(II) and zinc(II) complexes retain their structures in solution, with no evidence found for interconversion between the two forms. The crystal structure of a decomposition product $[Zn_4L_2(pypz)_2(PO_4)][PF_6]_3$ shows that $[L]^-$ is also capable of a binucleating ($\kappa^4:\kappa^2$) co-ordination mode, and provides a rare example of hydrolysis of $[PF_6]^-$ to $[PO_4]^{3-}$ under ambient conditions.

Acknowledgements

We thank the EPSRC for financial support, and Dr Peter Thornton of Queen Mary and Westfield College, London, for the magnetic susceptibility measurement on $[CoL][PF_6]$.

References

- 1 D. Philp and J. F. Stoddart, *Angew. Chem., Int. Ed. Engl.*, 1996, **35**, 1155; D. S. Lawrence, T. Jiang and M. Levett, *Chem. Rev.*, 1995, **95**, 2229; D. B. Amabilino and J. F. Stoddart, *Chem. Rev.*, 1995, **95**, 2725; J.-M. Lehn, *Supramolecular Chemistry*, VCH, Weinheim, 1995; A. F. Williams, *Chem. Eur. J.*, 1997, **3**, 15.
- 2 P. N. W. Baxter, J.-M. Lehn, J. Fischer and M.-T. Youinou, *Angew. Chem., Int. Ed. Engl.*, 1994, **33**, 2284; G. S. Hanan, D. Volkmer, U. S. Schubert, J.-M. Lehn, G. Baum and D. Fenske, *Angew. Chem., Int. Ed. Engl.*, 1997, **36**, 1842; P. Baxter, J.-M. Lehn, A. De Cian and J. Fischer, *Angew. Chem., Int. Ed. Engl.*, 1993, **32**, 69; D. M. Bassani, J.-M. Lehn, K. Fromm and D. Fenske, *Angew. Chem., Int. Ed. Engl.*, 1998, **37**, 2364.
- 3 R. W. Saalfrank, N. Löw, F. Hampel and H.-D. Stachel, *Angew. Chem., Int. Ed. Engl.*, 1996, **35**, 2209; R. W. Saalfrank, R. Burak, A. Breit, D. Stalke, R. Herbst-Irmer, J. Daub, M. Porsch, E. Bill, M. Müther and A. X. Trautwein, *Angew. Chem., Int. Ed. Engl.*, 1994, **33**, 1621.
- 4 T. Beissel, R. E. Powers and K. N. Raymond, *Angew. Chem., Int. Ed.*

- Engl.*, 1996, **35**, 1084; D. L. Caulder, R. E. Powers, T. N. Parac and K. N. Raymond, *Angew. Chem., Int. Ed. Engl.*, 1998, **37**, 1840.
- 5 C. Brückner, R. E. Powers and K. N. Raymond, *Angew. Chem., Int. Ed. Engl.*, 1998, **37**, 1837.
- 6 G. Baum, E. C. Constable, D. Fenske, C. E. Housecroft and T. Kulke, *Chem. Commun.*, 1999, 195.
- 7 B. Hasenknopf, J.-M. Lehn, N. Boumediene, E. Leize and A. Van Dorselaer, *Angew. Chem., Int. Ed. Engl.*, 1998, **37**, 3265.
- 8 E. C. Constable, *Prog. Inorg. Chem.*, 1994, **42**, 67; in *Comprehensive Supramolecular Chemistry*, ed. J.-M. Lehn, Pergamon, Oxford, 1996, vol. 9, p. 213.
- 9 J. S. Fleming, K. L. V. Mann, C.-A. Carraz, E. Psillakis, J. C. Jeffery, J. A. McCleverty and M. D. Ward, *Angew. Chem., Int. Ed. Engl.*, 1998, **37**, 1279.
- 10 S. Trofimenko, *Chem. Rev.*, 1993, **93**, 943.
- 11 P. L. Jones, A. J. Amoroso, J. C. Jeffery, J. A. McCleverty, E. Psillakis, L. H. Rees and M. D. Ward, *Inorg. Chem.*, 1997, **36**, 10.
- 12 N. Armaroli, V. Balzani, F. Barigelletti, M. D. Ward and J. A. McCleverty, *Chem. Phys. Lett.*, 1997, **276**, 435.
- 13 A. J. Amoroso, J. C. Jeffery, P. L. Jones, J. A. McCleverty, P. Thornton and M. D. Ward, *Angew. Chem., Int. Ed. Engl.*, 1995, **34**, 1443.
- 14 P. L. Jones, J. C. Jeffery, J. P. Maher, J. A. McCleverty, P. H. Rieger and M. D. Ward, *Inorg. Chem.*, 1997, **36**, 3088; D. A. Bardwell, J. C. Jeffery, P. L. Jones, J. A. McCleverty and M. D. Ward, *J. Chem. Soc., Dalton Trans.*, 1995, 2921.
- 15 P. L. Jones, K. L. V. Mann, J. C. Jeffery, J. A. McCleverty and M. D. Ward, *Polyhedron*, 1997, **16**, 2435; A. J. Amoroso, J. C. Jeffery, P. L. Jones, J. A. McCleverty, E. Psillakis and M. D. Ward, *J. Chem. Soc., Chem. Commun.*, 1995, 1175.
- 16 SHELXTL 5.03, Siemens Analytical X-Ray Instruments, Madison, WI, 1995; SHELXTL PLUS and SHELXL 93, Siemens Analytical X-Ray Instruments, Madison, WI, 1993.
- 17 R. Hoffman, J. M. Howell and A. R. Rossi, *J. Am. Chem. Soc.*, 1976, **98**, 2484; D. L. Kepert, in *Comprehensive Coordination Chemistry*, eds. G. Wilkinson, R. D. Gillard and J. A. McCleverty, Pergamon, Oxford, 1987, vol. 1, p. 31; W. O. Gillum, R. A. D. Wentworth and R. F. Childers, *Inorg. Chem.*, 1970, **9**, 1825.
- 18 C. Wendelstorf and R. Krämer, *Angew. Chem., Int. Ed. Engl.*, 1997, **36**, 2791; M. B. Inoue, M. Inoue and Q. Fernando, *Inorg. Chim. Acta*, 1993, **209**, 35; A. A. Belal, P. Chaudhuri, I. Fallis, L. J. Farrugia, R. Hartung, N. M. Macdonald, B. Nuber, R. D. Peacock, J. Weiss and K. Wiegardt, *Inorg. Chem.*, 1991, **30**, 4397; H. Al-Sagher, I. Fallis, L. J. Farrugia and R. D. Peacock, *J. Chem. Soc., Chem. Commun.*, 1993, 1499; D. Funkemeier and R. Mattes, *J. Chem. Soc., Dalton Trans.*, 1993, 1313; M. R. Churchill and A. H. Reis, Jr., *Inorg. Chem.*, 1972, **11**, 1811.
- 19 E. Larsen, G. N. La Mar, B. E. Wagner, J. E. Parks and R. H. Holm, *Inorg. Chem.*, 1972, **11**, 2652.
- 20 K. L. V. Mann, E. Psillakis, J. C. Jeffery, L. H. Rees, N. C. Harden, J. A. McCleverty, M. D. Ward, D. Gatteschi, F. Totti, F. E. Mabbs, E. J. L. McInnes, P. C. Riedi and G. M. Smith, *J. Chem. Soc., Dalton Trans.*, 1999, 339.
- 21 E. R. Humphrey, N. C. Harden, L. H. Rees, J. C. Jeffery, J. A. McCleverty and M. D. Ward, *J. Chem. Soc., Dalton Trans.*, 1998, 3353.
- 22 See, for example, N. G. Connelly, T. Einig, G. G. Herbosa, P. M. Hopkins, C. Mealli, A. G. Orpen, G. M. Rosair and F. Viguri, *J. Chem. Soc., Dalton Trans.*, 1994, 2025; U. Bossek, G. Haselhorst, S. Ross, K. Wiegardt and B. Nuber, *J. Chem. Soc., Dalton Trans.*, 1994, 2041; S. Kitagawa, M. Kondo, S. Kawata, S. Wada, M. Maekawa and M. Munakata, *Inorg. Chem.*, 1995, **34**, 1455 and refs. therein.
- 23 H. R. Clark and M. M. Jones, *J. Am. Chem. Soc.*, 1970, **92**, 816; *Inorg. Chem.*, 1971, **10**, 28.
- 24 A. M. W. Cargill Thompson, D. A. Bardwell, J. C. Jeffery and M. D. Ward, *Inorg. Chim. Acta*, 1998, **267**, 239.
- 25 See, for example, M. Pohl, Y. Lin, T. J. R. Weakley, K. Nomiyama, M. Kaneko, H. Weiner and R. G. Finke, *Inorg. Chem.*, 1995, **34**, 767; R. Neier, C. Trojanowski and R. Mattes, *J. Chem. Soc., Dalton Trans.*, 1995, 2521; Y. Zhang, A. Clearfield and R. C. Haushalter, *Chem. Mater.*, 1995, **7**, 1221; X. Bu, P. Feng and G. D. Stucky, *J. Chem. Soc., Chem. Commun.*, 1995, 1337; V. Soghomonian, Q. Chen, Y. Zhang, R. C. Haushalter, C. J. O'Connor, C. Tao and J. Zubieta, *Inorg. Chem.*, 1995, **34**, 3509.